

1 Comparing solar inverter design rules to subhourly solar resource simulations

2 Mónica Zamora Zapata,¹ Kari Lappalainen,² Adam Kankiewicz,³ and Jan Kleissl⁴

3 ¹⁾*Departamento de Ingeniería Mecánica, Universidad de Chile, Santiago, RM, 8370458,*
4 *Chile*

5 ²⁾*Unit of Electrical Engineering, Tampere University, Tampere, 33720,*
6 *Finland*

7 ³⁾*Black & Veatch, Kansas City, MO, 64114, USA*

8 ⁴⁾*Department of Mechanical and Aerospace Engineering, University of California San*
9 *Diego, La Jolla, CA, 92093, USA*

10 (*mzamora@uchile.cl)

11 (Dated: 25 August 2023)

12 The input of a solar inverter depends on multiple factors: the solar resource, weather conditions,
13 and control strategies. Traditional design calculations specify the maximum current
14 either as 125% of the rated module current or as the maximum 3 hour average current from
15 hourly simulations over a typical year, neglecting extreme irradiance conditions: cloud
16 enhancement events that usually last minutes. Inverter power-limiting control strategies
17 usually prevent extreme events to cause strong currents at the inverter but in some cases,
18 they can fail, leading to high currents. In this study, we aim to report how frequent and
19 strong these high currents could be. We use 10 years of 1 minute data from 7 stations
20 across the United States to estimate the photovoltaic string output through modeling the
21 short-circuit current I_{sc} , and the maximum-power point current I_{mp} , and compare them to
22 traditional inverter design values. We consider different configurations: minutely to hourly
23 resolution; 5 min to 3 h averaging time intervals; monofacial and bifacial modules (with a
24 case of enhanced albedo); and 3 fixed-tilt angles and horizontal single-axis tracking. The
25 bifacial modules with enhanced albedo lead to the highest currents for 1 min data, exceeding
26 3 hour averages by 53% for I_{sc} and 38% for I_{mp} . The 3 hour average maxima surpass
27 the conservative 125% design rule for bifacial modules. Inverter ratings at either a 200% of
28 the rated current or 1.55 times the 3 hour maximum could withstand all events regardless
29 of control strategies.

30 **I. INTRODUCTION**

31 Solar photovoltaic (PV) plants have grown strongly in the past decade, reaching 738 GW of
32 installed capacity worldwide in 2021, and capacity is expected to double in the next 5 years¹.
33 As solar penetration continues to grow, one of the main challenges for grid integration is the
34 variability of the solar resource as manifested in diurnal cycles and quick changes that can occur
35 due to passing clouds. Clouds usually diminish the solar irradiance reaching the surface but clouds
36 can also augment it, in a process known as cloud or irradiance enhancement.

37 Irradiance enhancement typically occurs during broken cloud sky conditions², and is caused
38 by forward scattering on thin clouds and reflection on the sides of thick clouds^{3,4}, which not only
39 increases the global irradiance but also modifies its spectral distribution⁵. While locations with
40 high elevation near the Equator are expected to yield stronger overirradiance measurements, events
41 have been reported all over the world. The peak measurements include 1,891 W/m² in Colorado,
42 USA⁶ and 1,845 W/m² in Brazil²; higher latitudes are not free of these events: 1,528 W/m² were
43 measured in Norway⁷. All these values far exceed the standard testing conditions of 1000 W/m²
44 for PV modules, and can potentially result in high output currents as well as power, both of which
45 also depend on the operating module temperature and inverter control strategies^{8,9}. Irradiance
46 enhancement events last from seconds to minutes^{2,7,8} and can cover multiple kilometers¹⁰, which
47 can pose a problem for utility scale PV plants.

48 Inverters and the inverter strings (i.e., how many solar modules to connect in series) must be
49 designed and selected such that the weather conditions at the site of interest will not exceed their
50 rated capabilities. For this purpose, solar inverters have control strategies, and solar installations
51 include protection fuses. Power-limiting control strategies increase the operating voltage under
52 sustained high irradiance conditions in order to diminish the inverter input power, which as a
53 consequence also results in a reduced operating current. This control is performed together with
54 the MPPT (maximum power point tracker), meaning that it deviates from the maximum power
55 point current (I_{mp}). This type of control could fail in specific circumstances, or have a longer
56 time response compared to the fuses¹¹, causing an undesired protection action. Partial shading
57 conditions with cloud enhancement are particularly challenging and can lead to long-term inverter
58 deterioration⁸. Aside from the control strategy, fuses exist in combiner boxes after the PV modules
59 as well as on inverter DC inputs. Fuses are designed to blow when the current surpasses a given
60 limit, reacting in the span of milliseconds. Note that fuses must sustain temperatures of up to 80°C

Comparing solar inverter design rules to subhourly solar resource simulations

that develop inside IP rated enclosures, which can reduce their admissible current by factors of around 0.8². The implemented control strategies within inverters also have software limitations which may limit DC feeder current limits. In case of an over-current, meaning that either the control strategy and/or the fuse failed to prevent the condition, a major inverter fault occurs. While the actual frequency of over-current faults may not be high, due to control strategies as well as heterogeneity of the PV modules and module degradation, blown fuses and inverter faults have been observed in several operational PV plants², and are a major maintenance issue as both require manual intervention; the fuses have to be replaced, and inverters need to be reset, but there is typically no on-site staff.

There are some aspects in the design process that may result in having more frequent extreme conditions than anticipated. The first is related to the temporal resolution of the weather data. Irradiance enhancement events tend to last seconds or minutes^{2,12,13}, while solar PV design usually considers hourly data, completely missing short-lived high currents that could lead to over-current events. A second aspect that contributes to a higher risk of damage due to overirradiance is the recent trend of increasing inverter loading ratios (ILR or DC/AC ratio) due to the declining costs of PV modules, and ease of wiring and connections. Increasing ILR means connecting more PV modules to an inverter, which results in “clipping” or losing some power when the output of the PV modules surpasses the inverter power capacity on bright days. While these losses are thought to be compensated by a higher production during winter months and in cloudy conditions, recent measurements in Brazil suggest the opposite: undersized inverters can result in a lower annual energy generation due to overheating¹⁴.

The effect of time resolution has gained attention in the context of energy clipping. Kharait et al.¹⁵ used 1 month of 1 minute measurements at the NIST testing site in Gaithersburg, MD, to predict energy yield and clipping losses for ILRs of 1.1, 1.3, and 1.5. Simulations in SolarFarmer showed that energy yield grows while clipping losses diminish with coarser time resolution and lower ILR, and that sensitivities are larger with higher ILR. Parikh et al.¹⁶ expanded this study at the same site, for PV systems with tracking and ILR of 1.43. They used machine learning models to apply clipping loss correction factors on hourly data, reducing the PV generation bias error. Similarly, Anderson and Perry¹⁷ used 29 ground stations in the US with 1 min solar data, and calculated correction factors for the clipping error of 30 min satellite data on a system with fixed tilt. This dataset was then used to train machine learning predictions in order to create a correction factor map for the continental US. This study considered a PV system with a fixed

Comparing solar inverter design rules to subhourly solar resource simulations

93 tilt of 20° and ILR of 1.4. In a study unrelated to clipping but considering non-linear effects of
94 temporal averaging, Luoma et al.¹² used 1 second resolution data in San Diego, CA, to predict
95 energy losses due to the effect of time resolution on the effective inverter efficiency, showing that
96 10 second resolution is needed to capture the losses related to cloud enhancement events.

97 So far, these studies have not analyzed high irradiance events. The industry standard for veri-
98 fying inverter input conditions is described by Ladd¹⁸ in a SolarPro article. While the NEC 1999
99 rule introduced a 125% multiplier, meaning that the minimum short-circuit current for selecting
100 an inverter would be 1.25 times the short-circuit current of the PV modules, the NEC 2017 rule al-
101 lows simulating the local conditions on the PV modules and then using the highest 3 hour average
102 of the modeled short-circuit current as the maximum operating condition (as long as it is higher
103 than 70% of the value obtained with the 125% multiplier). But a 3 hour average will neglect cloud
104 enhancement events. To examine whether neglecting subhourly features is a matter of concern
105 with respect to the existing design rules, there is a need to use high resolution data and report the
106 strength and frequency of potentially high current events. The issue of high irradiance events is
107 expected to be of greater importance for bifacial modules due to the increase in diffuse irradiance
108 observed during cloud enhancement events. There is a brief mention of over-currents for bifacial
109 modules in the IEA Task 13 report¹⁹, where estimates of maximum PV module current at 1 min
110 resolution were reported to be 42% higher than the maximum 3 hour average, considering fixed
111 tilt conditions at 3 sites in the US.

112 In this work, we compare the solar industry standard sizing calculations to subhourly solar
113 resource simulations, and study the effect of time resolution on the simulated short-circuit and
114 maximum power point currents, at the scale of a PV string. We consider 10 years of data with 1
115 minute resolution at 7 SURFRAD sites in the continental US. Simulations are run in pvlib for two
116 PV system configurations with standard and bifacial modules, considering three tilt angles as well
117 as horizontal single axis tracking for a total of 12 scenarios. The paper is structured as follows:
118 Section II describes the data, PV systems, and the methods. Section III shows the simulated
119 results and their comparison to current industry standards, reporting the frequency and duration of
120 extreme events. Section IV contains the conclusions.

¹²¹ **II. DATA AND METHODS**

¹²² **A. Solar and weather data**

¹²³ We use solar and meteorological data from 7 SURFRAD stations: Bondville, IL, Boulder, CO,
¹²⁴ Desert Rock, NV, Fort Peck, MT, Goodwin Creek, MS, Penn State, PA, and Sioux Falls, SD; cor-
¹²⁵ responding to different climate conditions in the continental US. The data has 1 minute resolution,
¹²⁶ and we use historical records spanning 10 years from 2011 to 2020. The data is downsampled to
¹²⁷ coarser time resolutions of 5, 15, 30, and 60 minutes.

¹²⁸ **B. PV systems**

¹²⁹ We use two reference PV systems for our simulations including monofacial and bifacial mod-
¹³⁰ ules. Since our focus is on module output conditions, our results will consider the expected output
¹³¹ of a single PV string without an inverter control strategy. Typically, inverters are connected to
¹³² several strings with similar setup of PV modules that are wired in parallel or in series. Tradition-
¹³³ ally, strings had been identical for ease of design and construction, but strings are becoming more
¹³⁴ heterogeneous as more projects are developed in complicated terrains. Each string is protected by
¹³⁵ a separate fuse. Therefore a string is the relevant unit for examining over-currents.

¹³⁶ The first PV system, representing the monofacial case, is taken from Ladd¹⁸, with a total ca-
¹³⁷ pacity of 120 kW consisting of 4 inverters of 30 kW. Each inverter is fed by 5 strings of 19 Yingli
¹³⁸ YL330P-35b modules connected in series. The ILR for this system is 1.05, and the inverter has a
¹³⁹ maximum input voltage of 1,000 V and a maximum operation current of 66 A (13.2 A per string
¹⁴⁰ in our case). The Yingli PV module has a 15 A fuse.

¹⁴¹ The second PV system, representing the bifacial cases, is taken from Ayala Pelaez et al.²⁰; it
¹⁴² is a 200 kW DC system with 6 Chint 36 kW inverters. The bifacial modules are Silfab 285 W,
¹⁴³ and no details were reported regarding the number of modules per string nor the number of strings
¹⁴⁴ connected to the inverter, so we assume that each inverter is fed by 5 strings of 19 Silfab modules
¹⁴⁵ in series leading to 570 modules in total. Assuming a high bifacial gain (BG) of 15%, attainable
¹⁴⁶ in a single-axis tracking configuration for an albedo of 0.4²¹, the module power gives an estimated
¹⁴⁷ ILR of 0.84 which is low. The inverter has a maximum input voltage of 1,000 V and for 5 strings
¹⁴⁸ it allows a maximum input current of 14 A per string. This inverter has a 15 A fuse.

¹⁴⁹ Each PV system is simulated for the following configurations. We consider 3 fixed-tilt angles

Comparing solar inverter design rules to subhourly solar resource simulations

and a case with horizontal single axis tracking (HSAT). The fixed-tilt angles are 10°, 25°, and an optimal tilt for each site. The optimal tilt corresponds to the angle that maximizes the energy yield for the monofacial module in the year 2020. The values obtained for each site are: Bondville, IL: 33°, Boulder, CO: 37°, Desert Rock, NV: 35°, Fort Peck, MT: 40°, Goodwin Creek, MS: 30°, Penn State, PA: 32°, and Sioux Falls, SD: 38°. For the bifacial modules, two albedo scenarios are considered: the annual mean of each site²², and an improved white painted concrete of 60%²³, as done in the IEA Task 13 report¹⁹. This enhanced albedo may not be realistic for traditional PV design, but we have included it to represent an extreme condition.

C. Simulation and current variables

We model the output from the PV modules using pvlib²⁴. Measured direct and diffuse solar irradiance is transformed to the plane of array using the Perez transposition model, and, depending on the case, either annual mean values of albedo or an enhanced albedo of 0.6 are given for the ground diffuse component²². Since both modules are in the CEC database, the expected module output is obtained with the single diode CEC model, which calculates the cell temperature using the NOCT (Nominal Operating Cell Temperature). Following Ladd¹⁸, all possible losses are set to zero (electrical, soiling, shading, and snow), representing the worst case scenario for current output without inverter control. For the bifacial system, the rear side irradiance is obtained with pvfactors, a 2D method for calculating the view factors for the back side irradiance²⁵. For bifacial irradiance, only data for elevation angles greater than 10° was considered for the search of maximum current, since some early times resulted in unrealistic high values. Eliminating these values is not expected to exclude real maximum currents since the highest overirradiance events occur near noon²⁶.

To compare our results with industry standards, we define the following output variables. The 125% multiplier from the NEC 2009 rule is applied to the module short-circuit current, $I_{sc,mod}$, which in these cases are 9.29 A for the Yingli and 9.49 A for the Silfab module: $I_{125\%} = 1.25 \cdot I_{sc,mod}$, corresponding to 11.61 A and 11.86 A, respectively.

In practice, we would use $I_{125\%}$ as the maximum operating condition per string to select an inverter. To reduce inverter cost, the NEC 2017 code allows reducing the conservative 125% value using a 3 hour average of simulated performance. We obtain the modeled (actual) short-circuit current with the single diode CEC model from pvlib: I_{sc} . In Ladd¹⁸, the short-circuit current was corrected using the cell temperature. Both methods yield similar results but their values are

Comparing solar inverter design rules to subhourly solar resource simulations

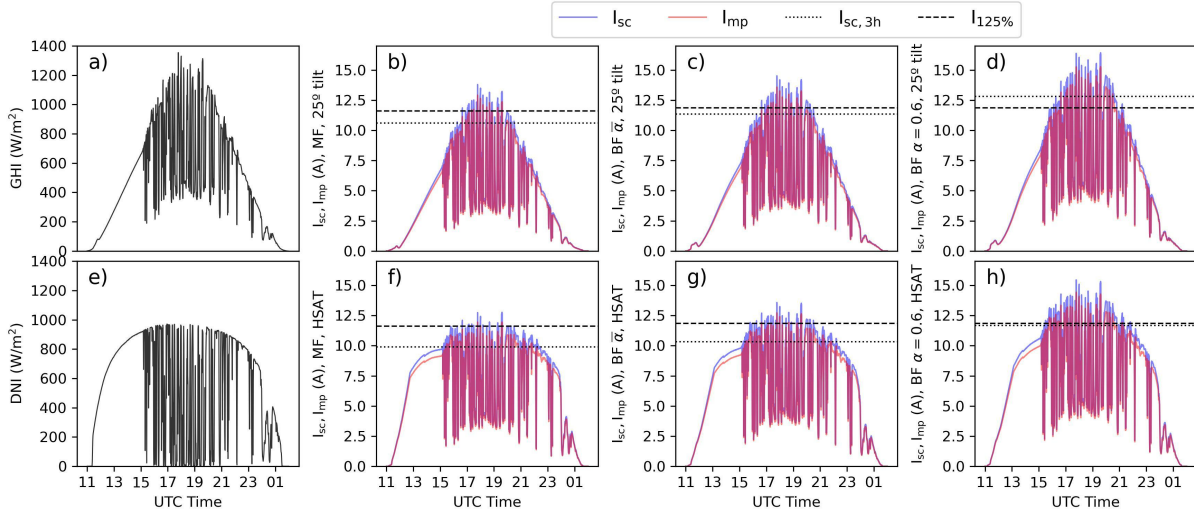


FIG. 1. Solar irradiance and modeled output currents for May 12, 2020 at Sioux Falls, showing strong variability for a large portion of the day. The first column shows the solar irradiance components: a) GHI (global horizontal irradiance) and e) DNI (direct normal irradiance). The modeled maximum-power point (red) and short-circuit (blue) currents are shown in the rest of the panels. The first row b-d) shows the values for the 25° tilt configuration and the second row f-h) for the HSAT configuration. The panels in the last three columns correspond to different module setups: b,f) show monofacial, c,g) bifacial with mean albedo, and d,h) bifacial with $\alpha = 0.6$. Horizontal lines correspond to the maximum current selected according to the 125% rule (dashed) and the maximum 3 hour average short-circuit current for the site (dotted).

sensitive to the module temperature coefficients α_{sc} and β_{oc} (not shown), which can slightly differ between the datasheet (used by Ladd) and the CEC database (used in pvlib). For consistency and reproducibility we use the CEC database and pvlib built-in methods. We also report values of the current at the maximum-power point, I_{mp} , which is the closest representation to typical operational conditions. For inverters with power-limiting control strategies, I_{mp} may be lower on bright days.

The NEC 2017 rule suggests using the maximum 3 hour average of the modeled short-circuit current, $I_{sc,3h}$. We will compare the average modeled short-circuit current and maximum-power current for different input data time resolutions as well as different averaging time windows: 5 min, 15 min, 30 min, 1 h and 3 h, for each of the sites, tilts, and module configurations.

189 **III. RESULTS**

190 **A. Sample results**

191 Fig. 1 shows the solar resource and the modeled short-circuit current (I_{sc}) as well as the mod-
 192 eled maximum-power point current (I_{mp}) for May 12, 2020, at Sioux Falls, SD. This day has strong
 193 variability, and irradiance enhancement events between 15:00-22:00 UTC.

194 The modeled I_{sc} and I_{mp} currents are shown for the 25° tilt configuration (Fig. 1b-d), which
 195 closely follow the global horizontal irradiance (GHI, Fig. 1a), while the HSAT results (Fig. 1f-h)
 196 resemble more the direct normal irradiance (DNI, Fig. 1e). The short-circuit current, I_{sc} , is by
 197 definition always greater than the maximum-power point current, I_{mp} . The modeled currents are
 198 amplified with bifacial modules, even more so when the albedo is enhanced, since the effective
 199 irradiance reaching the modules increases. With tracking, the current peaks are lower than those
 200 of the 25° fixed-tilt system throughout the day because horizontal tracking occurs at a suboptimal
 201 tilt angle. If we had considered tilted tracking, it would have resulted in more extreme values but
 202 two-dimensional tracking is uncommon for utility-scale plants. Lastly, the dashed and dotted lines
 203 show the selected maximum current by using the 125% rule and the 3 hour average, respectively.
 204 The modeled current peaks do surpass the industry standards at times, and can even be greater than
 205 15 A, the fuse rating, for some configurations. Lastly, we note that the maximum 3 hour average
 206 can be greater than the 125% rule for the bifacial modules with enhanced albedo.

207 **B. Maximum expected current and time resolution**

208 The effect of time resolution and the averaging time interval on the maximum I_{sc} is shown
 209 in Fig. 2 for Sioux Falls. All sites show a similar behavior: the maximum currents decrease
 210 when increasing the averaging time interval, as expected. Meanwhile, for the same averaging
 211 time interval, the maximum currents found for coarser time resolution are lower or equal than
 212 the maximum found for the 1 minute averaged at that time interval. This is also expected since
 213 the downsampled timeseries may lose some extreme information while the 1 minute averaged
 214 timeseries will always contain the highest peaks, leading to the highest possible maximum.

215 In other words, coarser time resolution can underestimate the maximum values, and averaging
 216 with longer time windows certainly underestimates them. However, the difference of time reso-
 217 lution is minor when looking at 3 hour statistics, meaning that the maximum value of the 3 hour

Comparing solar inverter design rules to subhourly solar resource simulations

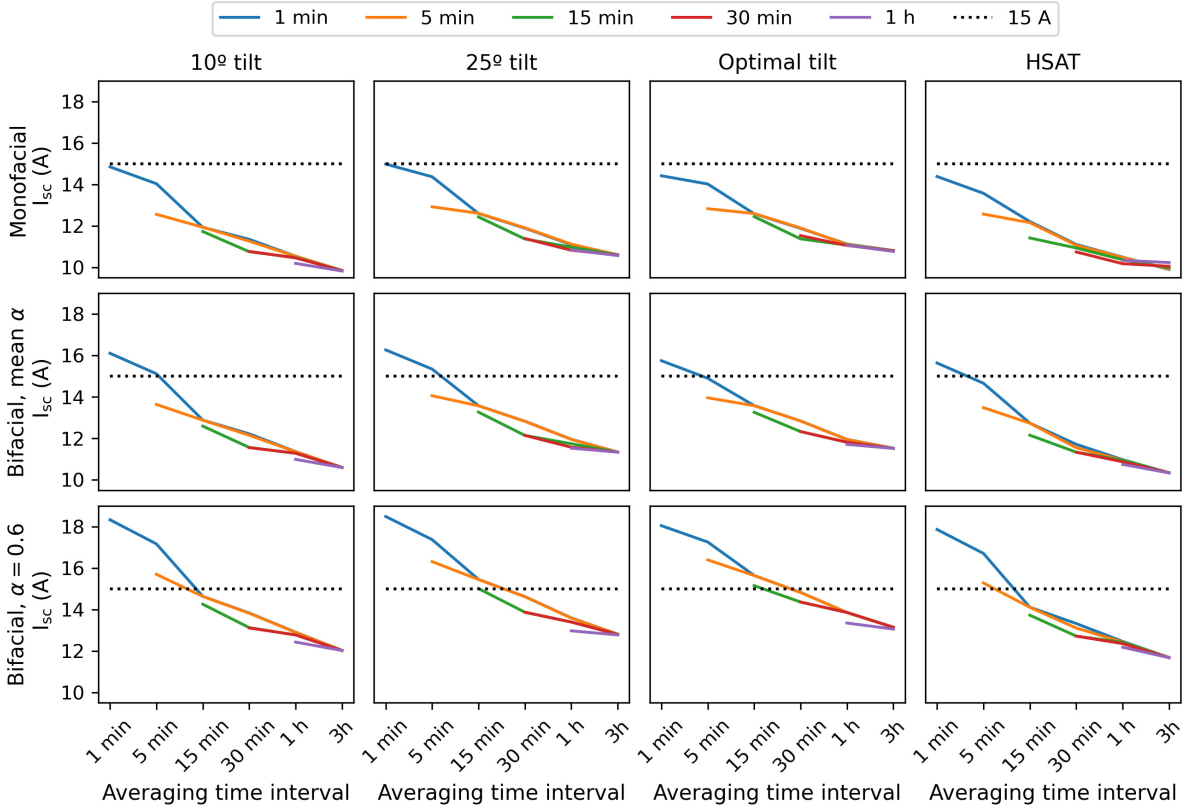


FIG. 2. Maximum short-circuit current I_{sc} for Sioux Falls, obtained from the different downsampled time-series (1 min to 1 h), are shown as a function of the averaging time interval (1 min to 3 h).

average, used for the NEC 2017 rule, is virtually identical if the original data has 1 minute or 1 hour resolution. The behavior of I_{sc} and I_{mp} is similar, with the latter being always lower by around 1.5 A (see Appendix A for complementary figures).

Fig. 3 presents the results of the 1 minute timeseries of maximum modeled short-circuit current as a function of averaging time interval for all sites. In other words, the 12 tilt/tracking and bi/monofacial cases considered in Fig. 2 are put together in a single plot for each site. The top row in Fig. 3 shows that the modeled maximum 1 minute short-circuit current for many configurations surpasses the inverter nameplate limits (13.2 A for the monofacial, 14 A for the bifacial, and also the 15 A fuses for the monofacial module and the Chint inverter).

Bifacial modules reach a higher current than monofacial ones, and the enhanced albedo creates the strongest maxima for the 25° tilt. The way in which maximum currents decrease with coarser averaging time intervals is unique for each site. Some sites show a more linear behavior while others suddenly decrease at a specific averaging time interval. In the case of Sioux Falls (and

Comparing solar inverter design rules to subhourly solar resource simulations

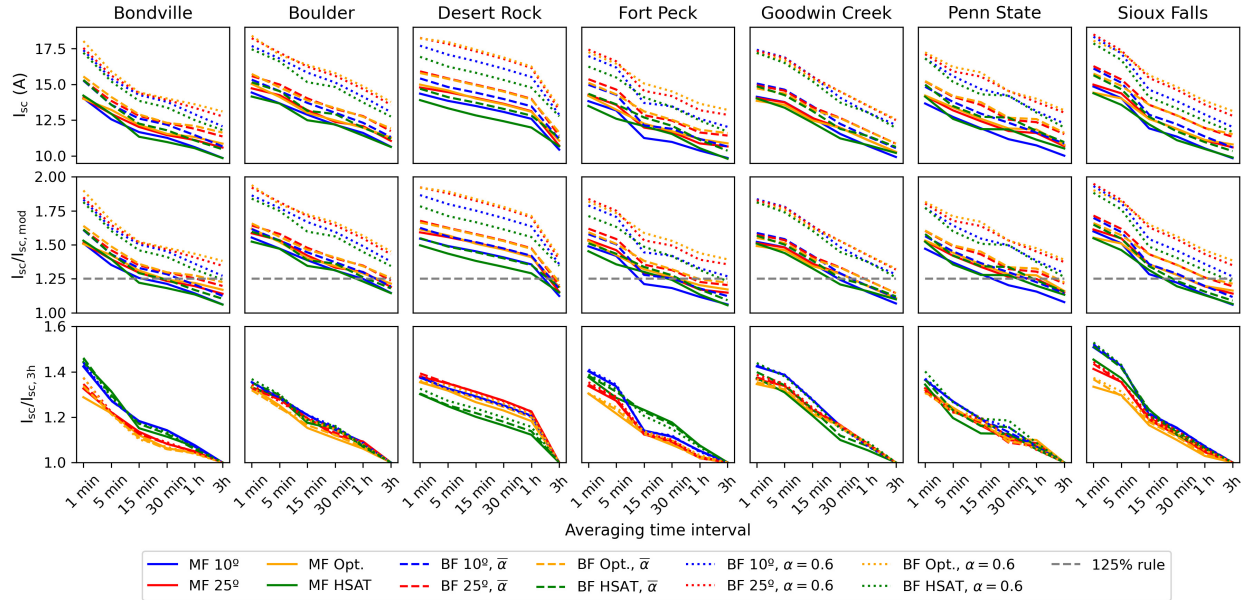


FIG. 3. Maximum modeled short-circuit current I_{sc} as a function of the averaging time interval by site, using the 1 minute resolution data. The top row shows the absolute values, the middle row shows the values normalized by the module short-circuit current $I_{sc,mod}$ with the 125% NEC in dashed gray. The bottom row shows the values normalized by the 3 h average maximum.

also Fort Peck in Fig. 3), the sudden decrease occurs between the 5 and 15 minute intervals. This difference suggests that there is a characteristic timescale related to the duration of the strong current events for each site, which is likely to be related to the features of the clouds that lead to the strongest irradiance enhancement events at each location. Fig. 3 shows that the longest timescale is seen for Desert Rock, where the change of slope occurs at the averaging time interval of 1 h.

The normalized current values (second and third rows in Fig. 3) show the ratio with respect to the module's reference short-circuit current, $I_{sc,mod}$, and the ratio with respect to the 3 hour average maximum, $I_{sc,3h}$ to comparing to the NEC 2009 and NEC 2017 calculations. The same plot is included for I_{mp} in Appendix A (Fig. 7).

The ratio $I_{sc}/I_{sc,mod}$ (Fig. 3 second row) shows that for all the bifacial modules with enhanced albedo, even the maximum 3 h average is greater than $I_{125\%}$, meaning that the 125% rule may not be conservative enough for those conditions, specially if the inverter has no control strategies. Furthermore, the 125% rule is not much greater than the 3 hour averages for Boulder and Desert Rock in the case of monofacial modules. Second, the maximum for the 1 minute data is almost double $I_{sc,mod}$ for Sioux Falls (195%), Boulder (194%), Desert Rock (192%) and Bondville (190%) in the

bifacial cases with enhanced albedo, while for the other cases the 1 minute maximum is at least 145% of $I_{sc,mod}$. For $I_{mp}/I_{sc,mod}$ (Fig. 7 second row), the values are less extreme but still surpass 125%: while for monofacial modules $I_{mp}/I_{sc,mod}$ ranges from 138% at Penn State to 151% at Boulder, the maximum values for bifacial modules reach 179% at Bondville and 178% at both Boulder and Desert Rock.

The bottom row in Fig. 3 shows the ratio between the maximum averaged values and the maximum 3 hour average value. Here, we see that with normalization, the curves become similar and dependent only of tilt or tracking configuration, which is expected since they determine the effective irradiance reaching the modules. The $I_{sc}/I_{sc,3h}$ ratio is greatest for the Sioux Falls site, where the 1 minute maximum is 53% greater than the maximum 3 h average, followed by Bondville (46%) and Goodwin Creek (44%), all of these values occurring for bifacial modules with enhanced albedo and a HSAT configuration. Meanwhile, the minimum occurs for monofacial modules at Bondville (29%). These values are in line with the simulated conditions and sites included in the IEA Task 13 report¹⁹, where the same ratio reached 42% for fixed tilt conditions at 3 sites in the US. In the case of $I_{mp}/I_{sc,3h}$ (Fig. 7 bottom row), the maximum ratios reach 38% for Sioux Falls while the minimum is 20% for Penn State.

C. Frequency and duration of high current events

The fact that the 125% rule is exceeded dramatically seems concerning. However, the strength of the most extreme event in 10 years is not the only factor that affects the operation of the PV system. Other relevant metrics are how frequent the modeled high current events over the 125% rule are for each site, and how long they usually last. Figs. 4 and 5 show different statistics for the events whose modeled I_{sc} and I_{mp} surpass $I_{125\%}$, with I_{mp} being closer to operational conditions. The statistics in each plot include: the total time above $I_{125\%}$ in hours per year (first column), the maximum duration of these events in minutes (mid column), and the number of events per year (third column).

As expected, the high current events may occur more frequently for higher tilt angles (blue and yellow bars), and for the locations with a more abundant solar resource: Boulder and Desert Rock. While the modeled I_{sc} in a PV plant with monofacial modules at Goodwin Creek might surpass the 125% rule for around 2 hours per year, another at Boulder could reach 12 hours per year. As we change to bifacial modules with enhanced albedo, the frequency increases, reaching up to 456

Comparing solar inverter design rules to subhourly solar resource simulations

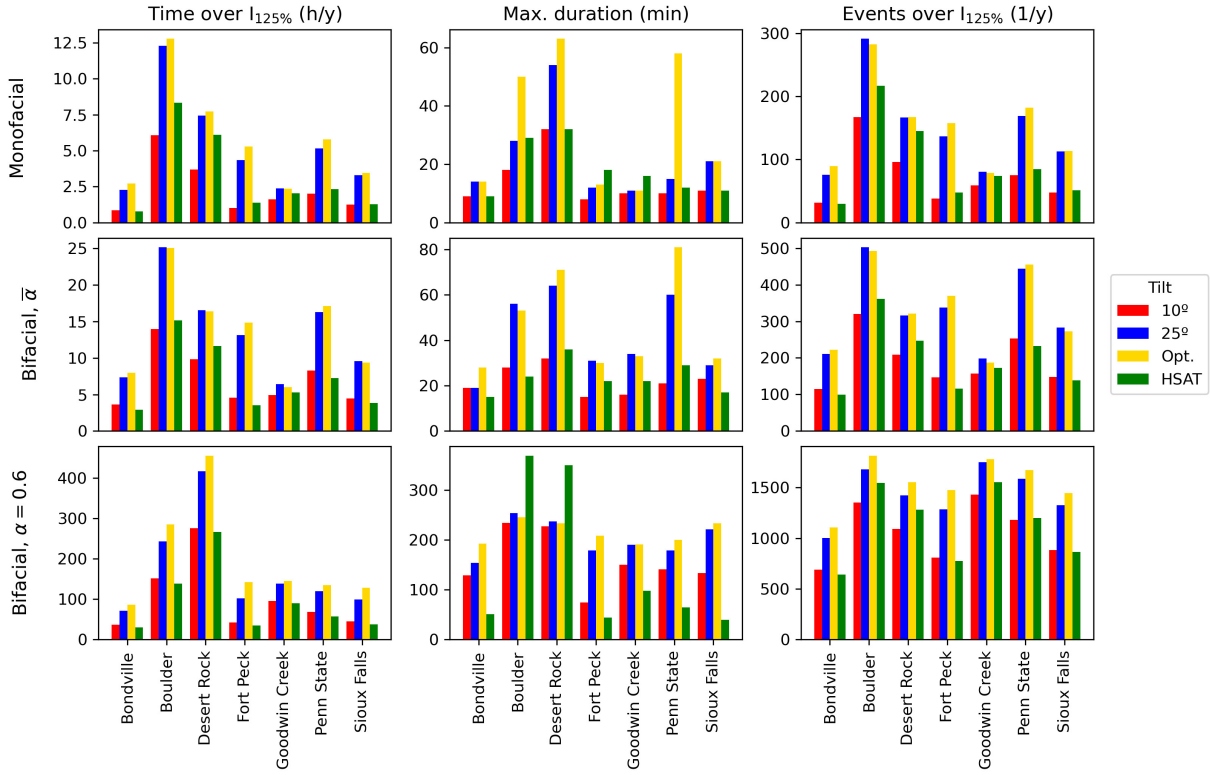


FIG. 4. Statistics of events whose short-circuit current is over the 125% rule per site and module configuration. The first column shows the aggregated time of these events per year, the second the maximum duration of the events, and the third the number of events per year. The first row corresponds to monofacial modules, the second to bifacial, and the bottom row to bifacial with enhanced albedo. The colors show the tilt or tracking configuration, with Opt. meaning optimal tilt angle.

276 hours per year at Desert Rock (equivalent to full 38 solar days). I_{mp} in Fig. 5 gives an idea of
 277 possible operational failures. The numbers are about a third of the statistics based on the modeled
 278 I_{sc} . The worst case in monofacial modules is Boulder with only 2.2 hours per year and bifacial
 279 with enhanced albedo at 134 hours (equivalent to 5.6 days).

280 In terms of duration, the longest events where the modeled $I_{sc} > I_{125\%}$ for the monofacial cases
 281 last between 8 and 63 minutes at Fort Peck and Desert Rock, respectively. For the bifacial modules
 282 with average site albedos, the range is between 15 minutes at both Bondville and Fort Peck, and
 283 81 minutes at Penn State. Lastly, the bifacial modules with enhanced albedo result in the longest
 284 events between 39 minutes for Sioux Falls and 369 (over 6 h) at Boulder, which are probably
 285 not related to irradiance enhancement but extended favorable conditions. In fact, note that the
 286 longest events for enhanced albedo occur at Boulder and Desert Rock for the HSAT configurations,

Comparing solar inverter design rules to subhourly solar resource simulations

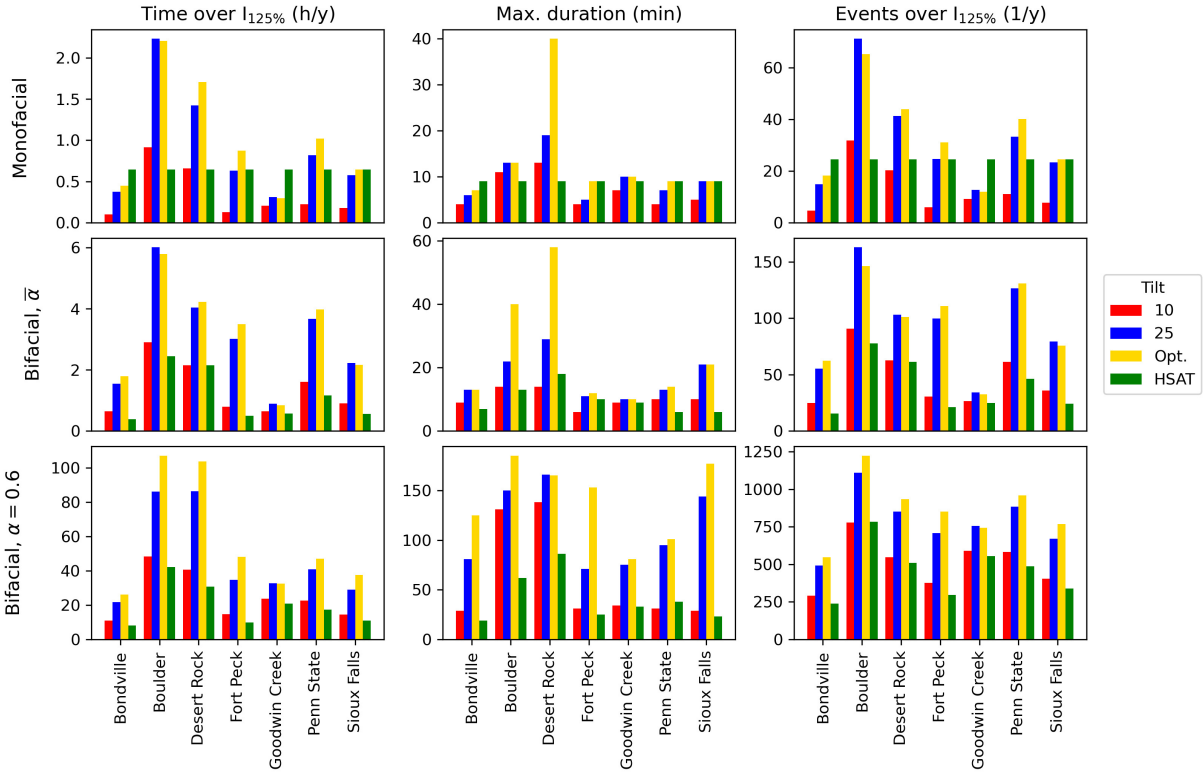


FIG. 5. Statistics of events whose maximum-power point modeled current is over the 125% rule per site and module configuration. The first column shows the aggregated time of these events per year, the second the maximum duration of single events, and the third the number of events per year. The first row corresponds to monofacial modules, the second to bifacial, and the bottom row to bifacial with enhanced albedo. The colors show the tilt or tracking configuration, with Opt. meaning optimal tilt angle.

meaning that tracking is playing an important role in augmenting the incident irradiance over the modules throughout the day, not just for irradiance enhancement events but mean irradiance as well. The extreme events based on modeled $I_{mp} > I_{125\%}$ show a similar behavior, but note that in these cases the longest events are not for the HSAT configuration. Here, the longest events last 40 min for the monofacial modules at Desert Rock, 58 min for the bifacial modules with site mean albedo at Desert Rock, and 185 min for the bifacial modules with enhanced albedo at Boulder. The maximum duration based on I_{mp} is around half that based on I_{sc} . As we previously saw in Fig. 3, the 125% rule determines a low requirement when comparing to the 3 h maximum average for bifacial modules with enhanced albedo, so the long duration of the events is also related to having too low of a threshold, in proportional terms.

Lastly, the number of events per year gives an idea of the possible maintenance frequency such

Comparing solar inverter design rules to subhourly solar resource simulations

as replacing fuses for inverters without control strategies. For both modeled I_{sc} and I_{mp} , Boulder leads for mono and bifacial modules, at either 25° or its optimal tilt setup. The maximum number of events for $I_{sc} > I_{125\%}$ are 291 for monofacial modules, 503 for bifacial with mean site albedo, and 1,816 for bifacial with enhanced albedo. Meanwhile, the maximum number of events for modeled $I_{mp} > I_{125\%}$ are 71 for monofacial modules, 163 for bifacial with mean site albedo, and 1,224 for bifacial with enhanced albedo. The number of extreme events based on modeled I_{mp} range between 24-67% of those based on I_{sc} .

Both the mean time over the 125% rule, the maximum duration of the extreme events, and the mean number of events per year help us to quantify the possible impact of the times where a PV string may deliver a strong current, complementing the previously provided maximum short-circuit current and maximum power-point current. This is especially important for some sites. While Sioux Falls presented the strongest 1 min maximum values, now we see that those events are not as frequent as in other locations like Boulder. Additional parameters related to frequency could also be helpful for inverter selection if the goal was to minimize the total time of failure instead of no failure at all in cases without power-limiting control strategies, or for choosing a tilt angle instead of a tracking system when working with bifacial modules.

IV. CONCLUSIONS

We have analyzed the possible impacts of overirradiance events in solar plants by reporting the frequency and duration of simulated high current outputs of a PV string and comparing them with inverter selection standards, considering several configurations and sites in the US. The study also covered the effect of time resolution and averaging on the modeled results. We used 10 years of 1 minute solar data for 7 sites in the SURFRAD network, and simulated the short-circuit and maximum-power point currents using pvlib. Modeled currents were compared with the industry standards NEC 2009 and NEC 2017, corresponding to the 125% rule and the 3 hour average maximum, respectively.

The maximum modeled short-circuit current decreases with time resolution and averaging and the shape of the decay varies by site. The 3 hour average maximum short-circuit current is insensitive to the original data time resolution. The 1 minute maximum short-circuit current was the strongest at Sioux Falls for the 25° tilt and bifacial module with enhanced albedo, and it greatly surpassed the 125% rule for all cases. In some cases, the 1 minute maximum even surpassed the

Comparing solar inverter design rules to subhourly solar resource simulations

328 inverter nameplate maximum and string fuses. For the bifacial modules with enhanced albedo, the
329 3 hour maximum was already greater than the 125% rule. This suggests that – even for coarse res-
330 olutions – 125% may not be a suitable rule for selecting an inverter without power-limiting control
331 for bifacial modules. The frequency of the events over the 125% rule was largest at the sites with
332 more solar resource: Boulder and Desert Rock. The longest extreme events were over 6 hour long
333 for bifacial modules with enhanced albedo and tracking.

334 The current industry standards for selecting inverters based on the 125% rule or 3 hour averages
335 were found to be lower than the maximum modeled currents caused by short and strong events of
336 overirradiance. While for monofacial modules the 3 hour average maximum is less strict than the
337 125% rule, this was not true for bifacial modules. If the goal was to create a rule that could avoid
338 any possible strong 1 minute event, either a 200% rule based on the module’s short-circuit current
339 or 1.5 times the 3 hour maximum average, which could be derived from hourly data, would avoid
340 any large current event. Still, if 1 min resolution data is available, either from measurements or
341 more recent satellite-derived commercial products, it will still be beneficial to do a high resolution
342 simulation for a more informed design.

343 We would like to note that the analysis performed used data that represents the behavior of a
344 single point in space. While a large solar plant is known to smooth the incoming strong irradiance
345 by geographic diversity effect related to covering a large area, single strings cover small subsets
346 of photovoltaic plants and do not experience spatial smoothing, following the results presented
347 herein.

348 Lastly, inverter power-limiting control deviates from the maximum-power point to higher volt-
349 age operating points^{8,10}, which usually leads to a lower operating current. Still, this type of control
350 strategies may fail under partial cloudy skies, and existing PV plants with maximum-power track-
351 ing algorithms are likely to continue failing. Future work could add realism to these type of
352 diagnostics by estimating the derating of fuses due to high temperatures, or to include an inverter
353 model in order to simulate the actual inverter input current.

354 ACKNOWLEDGMENTS

355 MZZ thanks the Faculty of Physical and Mathematical Sciences at Universidad de Chile for a
356 faculty incorporation grant. KL was funded by the Research Council of Finland (funding decision
357 348701).

358 **DATA AVAILABILITY STATEMENT**

359 Solar data are available at the SURFRAD website: <https://gml.noaa.gov/ftp/data/radiation/surfrad/>. The code used in this study is available at <https://github.com/mzamora/InverterEnhancement>.

360

361

362 **REFERENCES**

- 363 ¹International Energy Agency, “Renewables 2021,” Tech. Rep. (2021).
- 364 ²L. R. do Nascimento, T. de Souza Viana, R. A. Campos, and R. Rüther, “Extreme solar overirradiance events: Occurrence and impacts on utility-scale photovoltaic power plants in Brazil,” Solar Energy **186**, 370–381 (2019).
- 365
- 366
- 367 ³Z. K. Pecenak, F. A. Mejia, B. Kurtz, A. Evan, and J. Kleissl, “Simulating irradiance enhancement dependence on cloud optical depth and solar zenith angle,” Solar Energy **136**, 675–681 (2016).
- 368
- 369
- 370 ⁴G. H. Yordanov, “A study of extreme overirradiance events for solar energy applications using NASA’s I3RC Monte Carlo radiative transfer model,” Solar Energy **122**, 954–965 (2015).
- 371
- 372 ⁵M. A. Zamalloa-Jara, M. Sevillano-Bendezú, C. Ulbrich, G. Nofuentes, R. Grieseler, and J. A. Töfflinger, “Overirradiance conditions and their impact on the spectral distribution at low- and mid-latitude sites,” Solar Energy **259**, 99–106 (2023).
- 373
- 374
- 375 ⁶C. A. Gueymard, “Cloud and albedo enhancement impacts on solar irradiance using high-frequency measurements from thermopile and photodiode radiometers. Part 1: Impacts on global horizontal irradiance,” Solar Energy **153**, 755–765 (2017).
- 376
- 377
- 378 ⁷G. H. Yordanov, O.-M. Midtgård, T. O. Saetre, H. K. Nielsen, and L. E. Norum, “Overirradiance (cloud enhancement) events at high latitudes,” in *2012 IEEE 38th Photovoltaic Specialists Conference (PVSC) Part 2* (2012) pp. 1–7.
- 379
- 380
- 381 ⁸M. Järvelä and S. Valkealahti, “Operation of a PV power plant during overpower events caused by the cloud enhancement phenomenon,” Energies **13** (2020), 10.3390/en13092185.
- 382
- 383 ⁹K. Lappalainen and S. Valkealahti, “Experimental observations about the cloud enhancement phenomenon on PV strings,” in *8th World Conference on Photovoltaic Energy Conversion* (2022) pp. 1354 – 1358.
- 384
- 385

Comparing solar inverter design rules to subhourly solar resource simulations

- 386 ¹⁰K. Lappalainen and J. Kleissl, “Analysis of the cloud enhancement phenomenon and its effects
387 on photovoltaic generators based on cloud speed sensor measurements,” *Journal of Renewable*
388 and Sustainable Energy **12**, 043502 (2020).
- 389 ¹¹E. Bellini, “New study claims PV industry is neglecting overirradiance issues,” *PV Magazine*
390 International (2023).
- 391 ¹²J. Luoma, J. Kleissl, and K. Murray, “Optimal inverter sizing considering cloud enhancement,”
392 *Solar energy* **86**, 421–429 (2012).
- 393 ¹³M. Zamora Zapata, E. Wu, and J. Kleissl, “Irradiance enhancement events in the coastal stra-
394 tocumulus dissipation process,” in *Solar World Congress, Santiago, Chile, International Solar*
395 *Energy Society* (2019).
- 396 ¹⁴L. Toreti Scarabelot, G. Arns Raminelli, and C. R. Rambo, “Overirradiance effect on the
397 electrical performance of photovoltaic systems of different inverter sizing factors,” *Solar Energy*
398 **225**, 561–568 (2021).
- 399 ¹⁵R. Kharait, S. Raju, A. Parikh, M. A. Mikofski, and J. Newmiller, “Energy yield and clipping
400 loss corrections for hourly inputs in climates with solar variability,” in *2020 47th IEEE Photo-*
401 *voltaic Specialists Conference (PVSC)* (2020) pp. 1330–1334.
- 402 ¹⁶A. Parikh, K. Perry, K. Anderson, W. B. Hobbs, R. Kharait, and M. A. Mikofski, “Valida-
403 tion of subhourly clipping loss error corrections,” in *2021 IEEE 48th Photovoltaic Specialists*
404 *Conference (PVSC)* (2021) pp. 1670–1675.
- 405 ¹⁷K. Anderson and K. Perry, “Estimating subhourly inverter clipping loss from satellite-derived
406 irradiance data,” in *2020 47th IEEE Photovoltaic Specialists Conference (PVSC)* (2020) pp.
407 1433–1438.
- 408 ¹⁸C. Ladd, “Simulating NEC voltage and current values,” *Solar professional magazine* , 12–18
409 (2008).
- 410 ¹⁹J. Stein, C. Reise, J. B. Castro, G. Friesen, G. Maugeri, E. Urrejola, and S. Ranta, “Bifacial
411 photovoltaic modules and systems: Experience and results from international research and pilot
412 applications,” *Tech. Rep. (IEA, 2021)*.
- 413 ²⁰S. Ayala Pelaez, C. Deline, P. Greenberg, J. S. Stein, and R. K. Kostuk, “Model and validation
414 of single-axis tracking with bifacial PV,” *IEEE Journal of Photovoltaics* **9**, 715–721 (2019).
- 415 ²¹LG, “Bifacial design guide,” *Tech. Rep. (2017)*.
- 416 ²²B. Marion, “Albedo data sets for bifacial PV systems,” in *2020 47th IEEE Photovoltaic Special-*
417 *ists Conference (PVSC)* (2020) pp. 0485–0489.

Comparing solar inverter design rules to subhourly solar resource simulations

⁴¹⁸ ²³Solar World, “Calculating the additional energy yield of bifacial solar modules,” (2016).

⁴¹⁹ ²⁴W. F. Holmgren, C. W. Hansen, and M. A. Mikofski, “pvlib python: a python package for
⁴²⁰ modeling solar energy systems,” Journal of Open Source Software **3**, 884 (2018).

⁴²¹ ²⁵M. A. Anoma, D. Jacob, B. C. Bourne, J. A. Scholl, D. M. Riley, and C. W. Hansen, “View
⁴²² factor model and validation for bifacial PV and diffuse shade on single-axis trackers,” in *2017*
⁴²³ *IEEE 44th Photovoltaic Specialist Conference (PVSC)* (2017) pp. 1549–1554.

⁴²⁴ ²⁶A. Castillejo-Cuberos and R. Escobar, “Understanding solar resource variability: An in-depth
⁴²⁵ analysis, using Chile as a case of study,” Renewable and Sustainable Energy Reviews **120**,
⁴²⁶ 109664 (2020).

⁴²⁷ **Appendix A: Complementary statistics for I_{mp}**

⁴²⁸ The following Figs. 6 and 7 represent the same behavior shown for I_{sc} in Figs. 2 and 3 but for

⁴²⁹ the modeled maximum-power point current I_{mp} .

Comparing solar inverter design rules to subhourly solar resource simulations

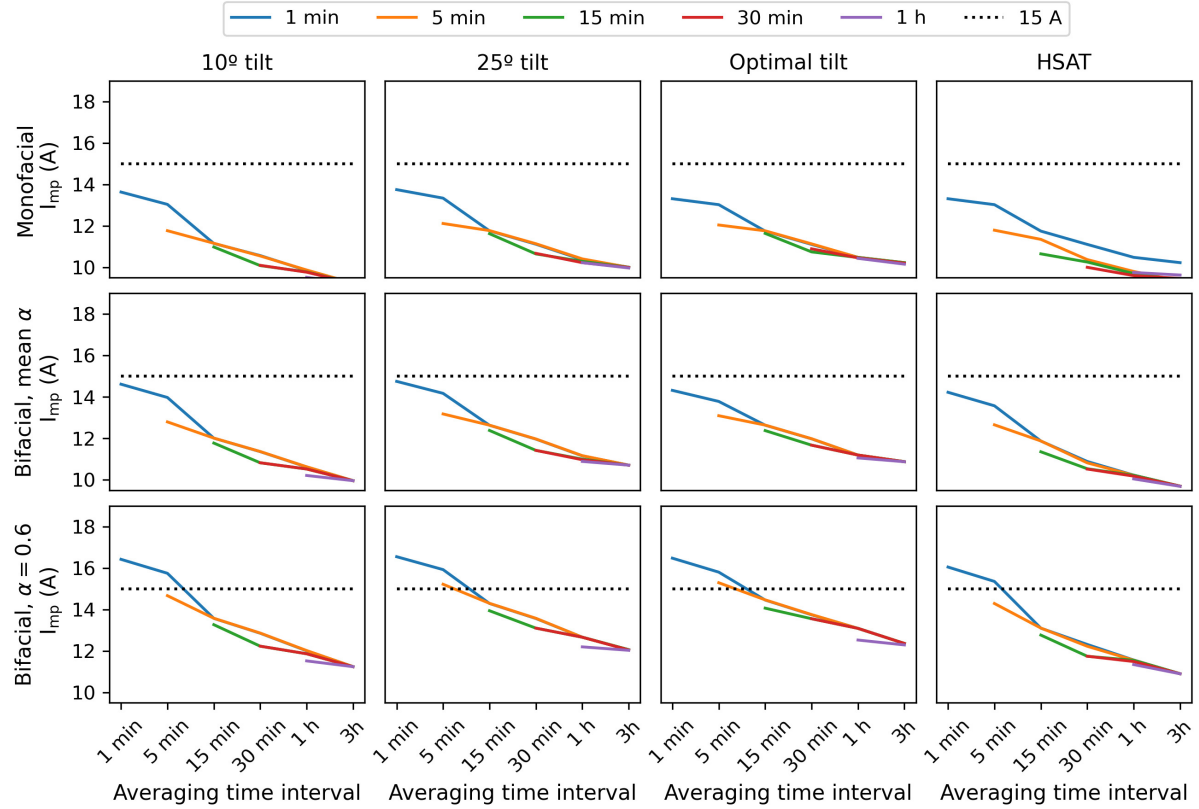


FIG. 6. Maximum current at the maximum-power point I_{mp} for Sioux Falls, obtained from the different downsampled timeseries (1 min to 1 h), are shown as a function of the averaging time window (1 min to 3 h).

Comparing solar inverter design rules to subhourly solar resource simulations

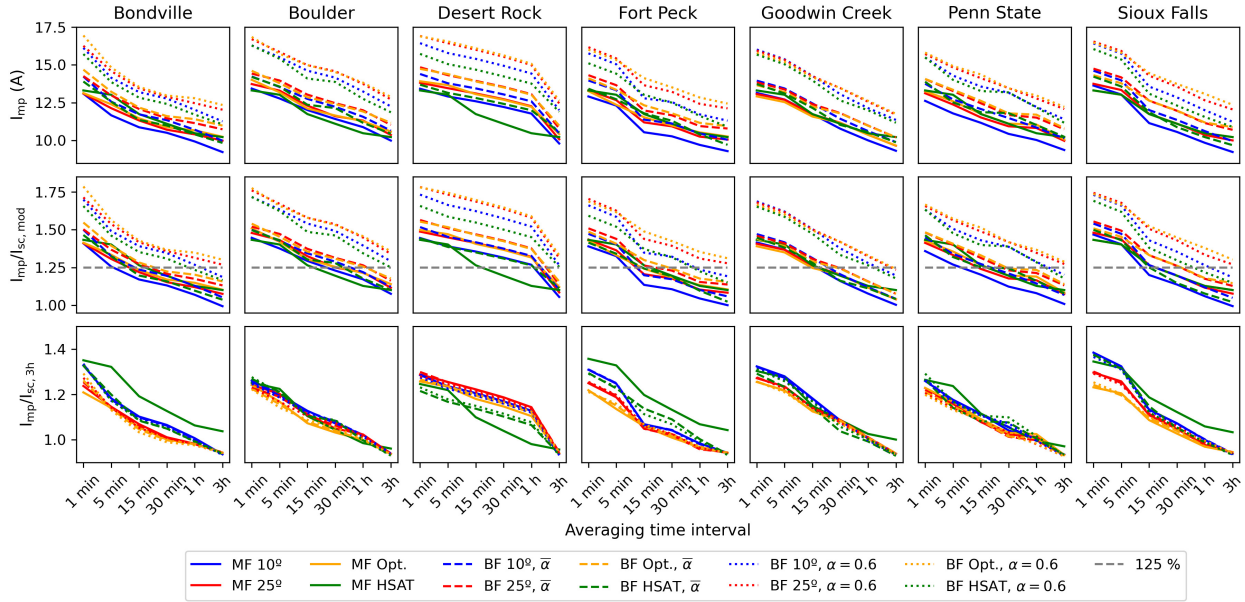


FIG. 7. Maximum current at the maximum-power point I_{mp} as a function of the averaging time window per site, using the 1 minute resolution data. The top row shows the absolute values, the middle row shows the values normalized by the module short-circuit current $I_{sc,mod}$ with the 125% NEC in dashed gray. The bottom row shows the values normalized by the 3 h average maximum.